ELSEVIER

Inorganica Chimica Acta 228 (1995) 173–185

Inorganica Chimica Acta

Crystal, molecular, electronic and vibrational structures of di-μ-thiocyanato-bis-[di-(3-aminopropyl)amine]-dicopper(II) diperchlorate

P.C. Christidis [a], C.A. Bolos [b], G. Bauer [c], G. Will [d], N.S. Trendafilova [e], G.St. Nikolov [e,f,*]

[a] *Laboratory of Applied Physics, Aristotle University, Thessaloniki 54006, Greece*
[b] *Department of Inorganic Chemistry, Aristotle University, Thessaloniki 54006, Greece*
[c] *Institute of General Chemistry, Technical University, Vienna 1060, Austria*
[d] *Institute of Mineralogy, University of Bonn, Bonn D-5300, Germany*
[e] *Institute of General and Inorganic Chemistry, Bulgarian Academy of Sciences, Sofia 1113, Bulgaria*
[f] *Department of Physical and Theoretical Chemistry, University of Plovdiv, Plovdiv 4000, Bulgaria*

Received 3 March 1994; revised 11 June 1994

Abstract

The crystal and molecular structures of the dimeric $[Cu(dpta)(NCS)(ClO_4)]_2$ (dpta = di(3-aminopropyl)amine) have been reinvestigated by X-ray diffraction. The crystals are orthorhombic, space group *Pbca* with $a = 13.938(3)$, $b = 12.424(3)$, $c = 15.864(2)$ Å, $V = 2747(1)$ Å^3 and $Z = 4$. The structure was refined to $R = 0.050$ ($R_w = 0.049$) from 1742 observed unique reflections. Each Cu atom is coordinated to the 3 N atoms of a dtpa ligand and to the N atom of an NCS^- group in an almost square planar arrangement. The Cu atom makes further axial contacts with the S atom of another $[Cu(dpta)(NCS)]^+$ unit and with one O atom of a ClO_4^- group thus forming a centrosymmetric dimeric unit $[(dpta)Cu^{NCS}_{SCN}Cu(dpta)]^{2+}$. Such units are held together by the ClO_4^- ions which provide Cu–O contacts and H bonds to neighbouring dpta H atoms. The ultimate arrangement around Cu may be described as a strongly elongated octahedron. The bond lengths (in Å) are: Cu–N(primary amine) = 1.999(6) and 2.012(6), Cu–N(secondary amine) = 2.052(5), Cu–N(NCS) = 2.000(6), Cu–S = 2.795(2), Cu–O = 2.93(1). Considering the plane of the two bridging NCS groups as equatorial, the dpta ligand is in a meridional position with chair–chair conformation in full agreement with molecular mechanics calculations. Chair–skew boat conformers, however, are predicted to lie close in energy. The IR and Raman spectra of the compound were assigned by normal coordinate analysis and MNDO calculations. The bands 855 (R), 890 (IR) and 980 (IR + R) cm^{-1} are typical for *mer*-coordinated dpta and can be used as a diagnostic tool to detect the ligand coordination mode.

Keywords: Crystal structures; Electronic structures; Vibrational structure; Copper complexes; Thiocyanate complexes; Amine complexes

1. Introduction

Acyclic polyamine ligands form numerous coordination compounds with Cu^{II} [1]. Among the tridentate polyamine ligands, the di-(2-aminoethyl)amine or 1,4,7-triazaheptane, also called diethylenetriamine (dien), and di-(3-aminopropyl)amine or 1,5,9-triazanonane, also called dipropylenetriamine (dpta), are of special interest mainly because they form with Cu^{II} stable compounds in which these ligands can adopt different conformations and take up different coordination sites. By making three contacts with Cu^{II} they leave one to three positions in the Cu coordination sphere which can be occupied by other unidentate or polydentate ligands in order to achieve four-, five- or six-coordination, respectively. Some examples of unidentate ligands which can play such a role are NCS^-, NO_3^-, Cl^-, Br^- and ClO_4^- [2–10]. In some cases NO_3^- is bridging and bidentate, increasing the coordination number of Cu^{II} to 5 [10]. Six-coordination usually occurs when two tridentate ligands are present simultaneously [9]. The N-coordinated NCS^- ligand is definitely the preferred unidentate ligand, but frequently it co-exists with NO_3^-

* Corresponding author; address e.

SSDI 0020-1693(94)04176-V

or ClO_4^- which are either outside (as counterions) [2] or inside [4–6] the Cu^{II} coordination sphere.

A marked difference exists between two [Cu(dpta)(NCS)X] compounds, depending on X. For $X=NO_3^-$, an almost square planar CuN_4 group is formed by the tridentate dpta and the N-coordinated NCS^- [2]. For $X=ClO_4^-$, however, dimerization occurs with two bridging NCS^- ligands and the ClO_4^- ion takes part in completing the coordination sphere to six [3,4]. Bridging NCS^- was found also in another dimer $[Cu(dien)(NCS)(ClO_4)]_2$ [6]. However, $[Cu(en)_2(NCS)(ClO_4)]$ is monomeric [8] with equatorial $[Cu(en)]^{2+}$ and axial NCS^-. Hence the trend to dimerization should not be related to the $NCS^- + ClO_4^-$ combination alone; the nature of the polydentate ligand with its ability to assume different conformations and form H bonds must play a major role. In this paper we shall explore this role.

The crystal and molecular structures of $[Cu(dpta)(NCS)(ClO_4)]_2$ have been previously reported [3,4]. These articles, however, do not describe the H bonds; the dpta conformation adopted after coordination was also not discussed in detail. In the absence of credible H bond data, the peculiar dimeric Cu coordination remains unclear. Hence more accurate structural parameters seem to be desirable especially in the presence of positional disorder in the studied compound (vide infra).

In this work we have re-investigated and refined the crystal and molecular structures of $[Cu(dpta)(NCS)(ClO_4)]_2$ in an attempt to reveal (i) why a simple substitution of NO_3^- by ClO_4^- can bring about such drastic structural changes, and (ii) what is the role of H bonds in shaping the dimer structure. Molecular mechanics (MM) calculations were used (a) to assess the relative stability of the conformers of coordinated dpta; (b) to find which dpta conformers are accessible with low energy and (c) to discriminate the preferred dpta coordination mode. An attempt has been made to interpret the complicated vibrational spectrum of the compound and to discern the regions that are most sensitive to the dpta coordination mode. Finally, the electronic structure of this compound was calculated in order to trace the effectiveness of the longer semi-coordinate Cu–S and Cu–O bonds and to get a glimpse at the nature of the Cu–N bonds.

2. Experimental

2.1. Preparation

To prepare the compound, 2.1 ml (20 mMol) benzaldehyde were mixed with 1.41 ml (10 mMol) 1,5,9-triazanonane and the resulting mixture was dissolved in methanol (50 ml). Further, 3.7 g of copper(II) perchlorate (**Caution**: perchlorate salt!), dissolved in methanol (20 ml), were added to this solution and the mixture was refluxed for 1 h. After cooling to room temperature, 0.76 g (10 mMol) ammonium thiocyanate dissolved in methanol was added. Blue crystals started to form after standing for 1 h and the crystallization process was complete after 12 h. The crystals were collected by filtration and dried under vacuum. The yield was 57%. *Anal.* Calc.: C, 23.86; H, 4.83; N, 15.91; Cu, 18.05. Found: C, 23.80; H, 4.84; N, 15.85; Cu, 17.95%. A Perkin-Elmer analyser was used to determine C, H and N. Copper was determined by atomic absorption spectroscopy.

2.2. Physical measurements

The magnetic moment, measured with a Gouy balance versus $[HgCo(SCN)_4]$ as calibrant was 1.80 BM.

The molar conductance for a 1 mMol solution in methanol was 180 $cm^2\ \Omega^{-1}\ mol^{-1}$, which indicates an 1:2 electrolyte.

The IR spectrum of the compound was measured with a Perkin-Elmer 225 spectrometer in KBr disks in the 400–4000 cm^{-1} range and in polyethylene disks in the 200–400 cm^{-1} range. The Raman spectrum was measured with a Bruker instrument in the 30–4000 cm^{-1} range.

The electronic spectrum, measured in a methanol solution, showed a very broad unresolved band at 16 700 cm^{-1} ($\epsilon = 271\ l\ cm^{-1}\ mol^{-1}$), and a narrow band at 28 900 cm^{-1}. It was similar to that reported for the $[Cu(dpta)(NCS)(NO_3)]$ solution [2] and should be attributed to absorption by the $[Cu(dpta)]^{2+}$ unit resulting upon dissociation into a 1:2 electrolyte (vide supra). The reflectance spectra displayed a band at 17 300 cm^{-1} (see also Ref. [11]) indicating that the species in solution and in the solid state have different coordination spheres.

2.3. X-ray measurements

A small blue crystal $0.25 \times 0.38 \times 0.42$ mm was mounted on a Rigaku AFC6R single-crystal diffractometer, equipped with a rotating anode. Cell parameters were obtained from direct measurements in the $23 < 2\theta < 26°$ range with Mo Kα monochromated radiation. Intensity data were collected up to $2\theta = 60°$. A total of 7294 reflections (excluding the standards) was measured and corrected for the intensity variation of the standard reflections as well as for the Lorentz and polarization effects but not for absorption. The corrected intensities were further averaged to produce 4000 unique reflections ($R_{int} = 0.03$) of which 1742 were considered as observed [$F_o > 5\sigma(F_o)$].

2.4. Structure refinements

The structure refinements and all the subsequent calculations were performed with the XTAL system [12]. Atomic scattering factors were taken from Ref. [13] and the anomalous dispersion corrections were adopted from the International Tables of Crystallography [14]. The atomic parameters of Cannas et al. [3] were used as starting ones. Three models were used in the refinement procedures:

Model 1. The structure refinement with all non-hydrogen atoms using unit statistical weights and isotropic temperature factors converged to $R=0.096$. In the next step anisotropic temperature factors were assigned to all but the oxygen atoms of the ClO_4^- groups, since the latter showed exceptionally large temperature factors. The new refinement converged at $R=0.073$. The difference Fourier map at this stage revealed around the Cl atoms four electron density maxima 1.7–2.0 e $Å^{-3}$ high at 1.35–1.45 Å distances. These peaks were assigned to the O atoms of a second ClO_4^- group orientation, i.e. positional disorder was assumed. Standard parameters of these atoms (O'(1)···O'(4)) and a common population parameter of 0.5 were introduced in the list of the least-squares variables. The same population parameter was assigned to the original O atoms (O(1)···O(4)).

The structure was further refined under the constraint $pp(O)+pp(O')=1$, i.e. only one independent population parameter was introduced. The R factor improved considerably, converging to 0.061. The population parameter value obtained at this stage was kept fixed in the subsequent calculations. Next, the H atoms could be identified in the difference Fourier map at positions near the calculated ones (C–H=0.95, N–H=0.95 Å). When the H atoms were included in the least-squares refinement and the restraints, based on the expected bonding geometries for these H atoms, the R value dropped to 0.051. Finally, the weighting scheme $w=1/\sigma^2(F)$ was introduced, where $\sigma^2(F)=\sigma^2(F)_{statistics}+\sigma^2(F)_{model}$ using the program REGWT of the XTAL system [12]. THe refinement converged to $R=0.050$, $R_w=0.049$, $GOF=0.981$, $[\Delta p/\sigma(p)]_{max}=1.056$ and $[\Delta p/\sigma(p)]_{av}=0.091$ for 229 variables. The maximal features in the final difference Fourier map were −0.7 and 0.8 e $Å^{-3}$ found in the region of the ClO_4^- group. An extinction correction was deemed as unnecessary.

Model 2. A second refinement was performed assuming an ordered ClO_4^- group as in the original paper of Cannas *et al.* [3]. Anisotropic temperature factors were assigned to the non-hydrogen atoms. Further, in order to obtain results comparable to those of the previous refinement, the H atom parameters were allowed to vary. The refinement converged smoothly, but the O atoms' thermal ellipsoids were abnormally large; some O atoms had semiaxes with r.m.s. values of up to 0.8 Å. The final results from this refinement were: $R=0.051$, $R_w=0.052$, $GOF=0.990$, $[\Delta p/\sigma(p)]_{max}=0.336$ and $[\Delta p/\sigma(p)]_{av}=0.033$ for 232 variables. The minima and maxima heights in the difference Fourier synthesis were −0.5 and 0.9 e $Å^{-3}$, respectively, found in the ClO_4^- group region.

Model 3. A third refinement was performed, assuming again an ordered ClO_4^- group but acentric space group ($Pbc2_1$), despite the fact that all the experimental evidence (e.g. systematic extinctions, intensity statistics) favoured the centric space group *Pbca*. Isotropic temperature factors were assigned to O and H atoms, anisotropic temperature factors were assigned to the other atoms. The results obtained were: $R=0.051$, $R_w=0.056$, $GOF=1.032$, $[\Delta p/\sigma(p)]_{max}=0.704$ and $[\Delta p/\sigma(p)]_{av}=0.066$ for 421 variables. The minima and maxima heights in the difference Fourier synthesis were −0.6 and 0.9 e $Å^{-3}$ respectively, found in the ClO_4^- group region. Refinements in the other two acentric subgroups of *Pbca*, i.e. $Pb2_1a$ and $P2_1ca$ gave identical results.

Choice of Model. By comparing the results from the three refinement models, it is seen that the acentric structure model should be excluded since (i) the 192 parameters introduced additionally in the refinement gave no significant improvement in the final residual factors; (ii) some bond lengths and valence angles appeared with unacceptable values. The choice between the first two models is difficult since both yielded essentially identical results. The involvement of all O atoms of the perchlorate group in H bonding and/or binding to the Cu atom (vide infra) favours an ordered arrangement of this group; it does not, however, rule out the possibility of a disordered ClO_4^- group. Similar cases are found in the literature (see, for example ND_4Br [15]). Following common practice in a similar situation and in the absence of any additional experimental evidence, we preferred to describe the structure with the first model, i.e. assuming a disordered ClO_4^- group. The atomic parameters and all the relevant structural data in this paper refer to this model. The fact that precision better than $R=0.05$ could not be reached, despite the high quality of our reflection data, should be attributed to the disordered state of the ClO_4^- group, for which only an approximate description can be given, as it is deduced from the relatively high residual electron density peaks, found in its region in all cases under consideration.

3. Computational procedures

The electronic structure of the free dpta ligand in different conformations was calculated with the MNDO program (MOPAC 6.0) [16]; no such calculation is possible for the Cu-containing fragments since param-

eters for Cu^{II} are lacking. The electronic structures of the $[CuNCS]^+$, $[Cu^{NCS}_{SCN}Cu]^{2+}$ and $[Cu(dpta)(NCS)]^+$ fragments were calculated using the ab initio GAMESS program [17] with a minimum basis set 3STO.

The different conformers of the free and Cu-coordinated dpta ligand were calculated by energy minimization using a molecular mechanics (MMX version) program [18]. MM applications have been described in detail elsewhere [19,20]. The MMX force field parameters used in the present calculations are discussed later in connection with the force field constants obtained from the vibrational analysis.

The vibrational spectra were assigned and the force field constants were extracted from the observed spectra by normal coordinate analysis (NCA) with a program using Cartesian coordinates [21]. The initial set of force constants was refined via a non-linear least-squares analysis between the calculated and observed vibrational frequencies. A VAX station 3100-M76 was used in the calculations. The MOPAC vibrational program after MNDO minimization [16] also helped assign the vibrational spectrum.

4. Results and discussion

4.1. Crystal and molecular structures from X-ray diffraction

The unit cell parameters are given in Table 1, final atomic coordinates and isotropic temperature factors are given in Table 2 and the intra- and intermolecular atomic distances and valence angles are given in Table 3.

The crystal and molecular structures of the studied compound reported here are essentially those of Cannas et al. [3,4]. Our cell parameters deviate 0.01 Å for c and 0.03 Å for b. In view, however, of the relatively high e.s.d.s of the former work, these differences are not statistically significant. Also, our bond lengths differ from those reported earlier on the average by about 0.02 Å and the valence angles by about 0.3 Å. For the same reason all these differences lie in general within experimental error $3\sigma_{combined}$. Since our e.s.d.s are on the average two times lower than those reported previously, several distinctions can be made, based on our data that could not be attempted with the former results (vide infra).

Table 1
Crystal data for $[Cu(dpta)(NCS)(ClO_4)]_2$

Formula	$(C_7H_{17}ClCuN_4O_4S)_2$
System	orthorhombic
Space group	*Pbca*
a (Å)	13.938(3)
b (Å)	12.424(3)
c (Å)	15.864(2)
V (Å^3)	2747(1)
Z	4
Formula weight	704.34
$F(000)$	1448
ρ_{calc} (mg m^{-3})	1.703
μ (cm^{-1})	19.47
λ(Mo Kα) (Å)	0.71069

A perspective view of the dimeric molecular unit with two neighbouring ClO_4^- groups is shown in Fig. 1. The Cu^{II} ion is bonded to the three dpta N atoms and to the thiocyanate N atom. The CuN_4 group is almost planar but not exactly square with Cu 0.178(1) Å above the 4N plane.

The coordination around the Cu^{II} atom is further completed by two intermolecular contacts above and below the CuN_4 plane: with the S atom from an already N-coordinated NCS^- group and with one O atom from a neighbouring ClO_4^- group. The two axial bonds are longer than usual and they correspond to the so-called semi-coordinate bonds [22,23]. The ultimate arrangement around Cu^{II} is that of a CuN_4SO octahedron strongly elongated along the O–Cu–S axis.

The double NCS^- bridge forms an essentially planar, rectangular eight-membered $Cu^{NCS}_{SCN}Cu$ ring (Fig. 2). Its mean plane contends a dihedral angle of 89.4(1)° with the CuN_4 plane, i.e. the two planes are almost perpendicular. The CuSC angle is 94.7(2)° which indicates that the CuS and SC bond vectors are almost perpendicular.

The NCS groups are not strictly linear: the NCS angle is 177.6(6)° and this is fully consistent with data reported for the corresponding NO_3^- compound (178.3(7)°). A slight deviation from linearity seems to be a common feature of N-coordinated NCS (see, e.g. Refs. [22,23]).

The Cu^{II}–Cu^{II} distance is 5.533(1) Å. Similar distances are typical for other Cu^{II} dimers with azide or oxalate bridging ligands [24] and magnetic exchange between the two Cu^{II} atoms is expected through the conjugated electron system [24].

4.2. DPTA conformation

The dpta ligand makes three contacts with Cu^{II}, forming two fused six-membered chelate rings N–CH_2–CH_2–CH_2–N–Cu. Taking the double bridge to be equatorial, dpta is in a *mer* position [25]. Both rings are in chair conformations. They are oriented with their central C parts towards oxygen atoms of two different ClO_4^- groups (Fig. 2) and thus they are expected to differ considerably with respect to the CuN^ACC torsional angles (58 and 47°). Here N^A denotes the primary amine N atom (see Table 3). Dihedral angles CuN^ACC lower than 60° suggest [19] that the chelate rings are distorted towards a skew boat con-

Table 2
Positional, isotropic displacement and site occupation parameters for $[Cu(dpta)(NCS)(ClO_4)]_2$

Atom	x	y	z	U	PP
Cu	0.48510(5)	0.18065(5)	0.60111(4)	0.0356(1)*	
C(1)	0.4308(4)	0.0685(5)	0.4309(4)	0.040(2)*	
C(2)	0.3455(6)	0.1033(6)	0.7329(6)	0.064(3)*	
C(3)	0.3827(6)	0.1828(7)	0.7963(4)	0.063(2)*	
C(4)	0.4900(6)	0.2049(5)	0.7893(3)	0.053(2)*	
C(5)	0.6199(5)	0.2964(6)	0.7197(5)	0.060(2)*	
C(6)	0.6591(5)	0.3565(6)	0.6462(6)	0.063(2)*	
C(7)	0.6824(5)	0.2851(7)	0.5721(6)	0.068(3)*	
N(1)	0.4418(4)	0.1180(5)	0.4914(4)	0.053(2)*	
N(2)	0.3560(4)	0.1420(5)	0.6469(4)	0.056(2)*	
N(3)	0.5187(4)	0.2606(4)	0.7103(3)	0.040(1)*	
N(4)	0.5934(4)	0.2440(5)	0.5335(4)	0.055(2)*	
S	0.4174(1)	0.0025(1)	0.3429(1)	0.0509(5)*	
Cl	0.3310(1)	0.0631(1)	0.0745(1)	0.0575(5)*	
O(1)	0.241(1)	0.054(1)	0.039(1)	0.112(4)	0.57(1)
O(2)	0.320(1)	0.115(1)	0.155(1)	0.125(5)	0.57
O(3)	0.3900(9)	0.133(1)	0.0253(8)	0.083(3)	0.57
O(4)	0.369(1)	−0.034(1)	0.108(1)	0.132(5)	0.57
O'(1)	0.341(1)	−0.052(2)	0.084(1)	0.102(5)	0.43
O'(2)	0.420(2)	0.106(3)	0.082(2)	0.17(1)	0.43
O'(3)	0.252(1)	0.120(2)	0.110(1)	0.107(5)	0.43
O'(4)	0.309(3)	0.049(3)	−0.011(2)	0.18(1)	0.43
H1(C2)	0.388(5)	0.043(5)	0.740(4)	0.06(2)	
H2(C2)	0.284(6)	0.092(6)	0.743(4)	0.09(3)	
H1(C3)	0.375(4)	0.147(5)	0.855(4)	0.05(2)	
H2(C3)	0.351(4)	0.249(5)	0.792(4)	0.06(2)	
H1(C4)	0.516(4)	0.143(6)	0.802(5)	0.07(2)	
H2(C4)	0.502(4)	0.244(5)	0.839(4)	0.05(2)	
H1(C5)	0.655(4)	0.239(5)	0.733(4)	0.05(2)	
H2(C5)	0.624(5)	0.342(6)	0.769(5)	0.08(3)	
H1(C6)	0.714(6)	0.400(7)	0.661(4)	0.09(3)	
H2(C6)	0.612(5)	0.418(6)	0.630(4)	0.07(3)	
H1(C7)	0.720(7)	0.219(8)	0.592(5)	0.15(5)	
H2(C7)	0.717(7)	0.329(8)	0.531(5)	0.15(5)	
H1(N2)	0.329(6)	0.097(7)	0.614(5)	0.11(3)	
H2(N2)	0.326(4)	0.194(5)	0.645(3)	0.05(2)	
H(N3)	0.488(4)	0.318(5)	0.708(3)	0.05(2)	
H1(N4)	0.610(4)	0.194(5)	0.498(4)	0.05(2)	
H2(N4)	0.572(3)	0.296(4)	0.505(3)	0.03(1)	

Asterisks indicate equivalent isotropic temperature factors, $U_{eq} = (1/3)\Sigma\Sigma U_{ij} a_i^* a_j^* a_i a_j$.

formation which must lie close in energy to the chair conformer (see also Section 4.6).

4.3. ClO_4^- geometry

Each ClO_4^- group contacts one Cu^{II} and makes several H bonds with the dpta ligand. Because of the exhibited disorder, the ClO_4^- geometry was of lower accuracy in comparison with that of the rest of the structure. However, within experimental error, the determined parameters are in agreement with those generally accepted [26].

4.4. Hydrogen bonds

The H bonds were not determined by Cannas et al. [3] although they list some O–C and O–N distances that were essential in evaluating the main contributions to the intermolecular repulsion. As seen from Table 3 and Fig. 2 all perchlorate O atoms participate in H bonding with the dpta's primary amine N and secondary amine N hydrogen atoms. The H1 atom bonded to N(2) bifurcates two H bonds with one and the same ClO_4^- group; H2 bonded to the same N(2) atom also bifurcates two H bonds with another ClO_4^- group but these bonds are shorter than those in which H1 is involved. The secondary amine H atom makes only one H bond with the ClO_4^- group which has already formed H bonds with H2 of N(2). This is the reason why the two H atoms of the amine group form inequivalent H bonds. The secondary amine H makes the smallest NH···O angle. There is no crystallographic equivalence between the two NH groups of one and the same dpta

Table 3
Selected intra- and intermolecular distances (Å) and angles (°) in $[Cu(dpta)(NCS)(ClO_4)]_2$

Cu–N(1)(NCS)	2.000(6)	N(3)–Cu–O(3)^{ii}	93.8(3)
Cu–N(2)(amine)	1.999(6)	N(3)–Cu–O′(2)^{ii}	73.0(7)
Cu–N(3)(sec. amine)	2.052(5)	N(4)–Cu–O(3)^{ii}	79.1(3)
Cu–N(4)(amine)	2.012(6)	N(4)–Cu–O′(2)^{ii}	79.5(7)
S–C(1)	1.631(6)	S^{i}–Cu–N(1)	96.1(2)
C(1)–N(1)	1.150(8)	S^{i}–Cu–N(2)	97.3(2)
N(2)–C(2)	1.45(1)	S^{i}–Cu–N(3)	90.9(1)
C(2)–C(3)	1.50(1)	S^{i}–Cu–N(4)	97.1(2)
C(3)–C(4)	1.52(1)	S^{i}–Cu–O(3)^{ii}	174.2(2)
C(4)–N(3)	1.486(8)	S^{i}–Cu–O′(2)^{ii}	163.0(7)
N(3)–C(5)	1.487(9)	Cu–S–C(1)	94.7(2)
C(5)–C(6)	1.49(1)	S–C(1)–N(1)	177.6(6)
C(6)–C(7)	1.51(1)	C(1)–N(1)–Cu	167.0(6)
C(7)–N(4)	1.47(1)	Cu–N(2)–C(2)	120.7(5)
		N(2)–C(2)–C(3)	112.1(6)
N(1)–Cu–N(2)	87.2(3)	C(2)–C(3)–C(4)	114.1(6)
N(1)–Cu–N(3)	172.9(2)	C(3)–C(4)–N(3)	114.1(6)
N(1)–Cu–N(4)	85.1(2)	C(4)–N(3)–Cu	115.2(4)
N(1)–Cu–O(3)^{ii}	79.3(3)	C(5)–N(3)–C(5)	108.1(5)
N(1)–Cu–O′(2)^{ii}	100.2(7)	C(5)–N(3)–Cu	116.5(4)
N(2)–Cu–N(3)	90.9(2)	N(3)–C(5)–C(6)	114.8(6)
N(2)–Cu–N(4)	164.4(3)	C(5)–C(6)–C(7)	113.3(6)
N(2)–Cu–O(3)^{ii}	86.1(3)	C(6)–C(7)–N(4)	110.2(6)
N(2)–Cu–O′(2)^{ii}	88.5(7)	C(7)–N(4)–Cu	123.1(5)
N(3)–Cu–N(4)	95.1(2)		
Cl–O(1)	1.39(2)	O(1)–Cl–O(4)	115(1)
Cl–O(2)	1.43(2)	O(2)–Cl–O(3)	106(1)
Cl–O(3)	1.43(1)	O(2)–Cl–O(4)	95(1)
Cl–O(4)	1.42(2)	O(3)–Cl–O(4)	120(1)
Cl–O′(1)	1.45(2)	O′(1)–Cl–O′(2)	107(2)
Cl–O′(2)	1.35(3)	O′(1)–Cl–O′(3)	121(1)
Cl–O′(3)	1.43(2)	O′(1)–Cl–O′(4)	90(2)
Cl–O′(4)	1.39(4)	O′(2)–Cl–O′(3)	118(2)
		O′(2)–Cl–O′(4)	110(2)
O(1)–Cl–O(2)	108(1)	O′(3)–Cl–O′(4)	106(2)
O(1)–Cl–O(3)	110(1)		

Intermolecular contacts

Cu···S^{i}	2.795(2)	S···N(1)^{i}	2.779(6)
Cu···O′(2)^{ii}	2.82(3)	C(1)···N(1)^{i}	3.169(9)
Cu···O(3)^{ii}	2.93(1)	C(1)···C(1)^{i}	3.379(8)

Hydrogen bonds	D–H (Å)	H···A (Å)	D···A (Å)	D–H···A (°)
N(2)–H1(N2)···O(1)^{iii}	0.85(8)	2.43(8)	3.27(2)	170(7)
N(2)–H1(N2)···O′(1)^{iii}	0.85(8)	2.48(8)	3.12(2)	133(7)
N(2)–H1(N2)···O(4)^{iii}	0.85(8)	2.87(8)	3.46(2)	128(7)
N(2)–H2(N2)···O(2)^{ii}	0.77(6)	2.38(7)	3.07(2)	149(6)
N(2)–H2(N2)···O(3)^{ii}	0.77(6)	2.58(7)	3.34(2)	167(6)
N(3)–H(N3)···O′(2)^{ii}	0.83(6)	2.40(6)	2.96(3)	125(5)
N(3)–H(N3)···O(2)^{ii}	0.83(6)	2.62(6)	3.29(2)	139(5)
N(4)–H1(N4)···O(1)^{ii}	0.87(6)	2.59(6)	3.33(2)	144(5)
N(4)–H1(N4)···O(3)^{ii}	0.87(6)	2.78(6)	3.53(2)	145(5)

Torsional angles	
Cu–N(2)–C(2)–C(3)	58.3(7)
N(2)–C(2)–C(3)–C(4)	−63.3(8)
C(2)–C(3)–C(4)–N(3)	66.5(8)
C(3)–C(4)–N(3)–Cu	−59.2(7)
C(4)–N(3)–Cu–N(2)	42.6(5)
N(3)–Cu–N(2)–C(2)	−44.1(6)
Cu–N(3)–C(5)–C(6)	50.0(7)
N(3)–C(5)–C(6)–C(7)	−75.1(9)
C(5)–C(6)–C(7)–N(4)	70.1(9)
C(6)–C(7)–N(4)–Cu	−47.0(8)
C(7)–N(4)–Cu–N(3)	24.6(6)
N(4)–Cu–N(3)–C(5)	−23.9(5)

Symmetry operations: $^{i}1-x, -y, 1-z$; $^{ii}x, \frac{1}{2}-y, \frac{1}{2}+z$; $^{iii}\frac{1}{2}-x, -y, \frac{1}{2}+z$; $^{iv}\frac{1}{2}+x, y, \frac{1}{2}-z$; $^{v}1-x, -\frac{1}{2}+y, \frac{1}{2}-z$.

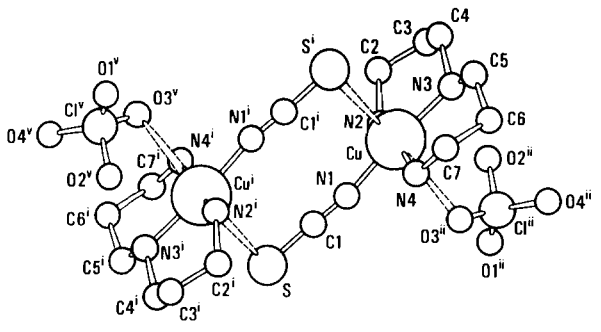

Fig. 1. The dimeric molecular unit of $[Cu(dpta)(NCS)]_2^{2+}$ with two neighbouring ClO_4^- groups. For the symmetry operations involved see Table 3.

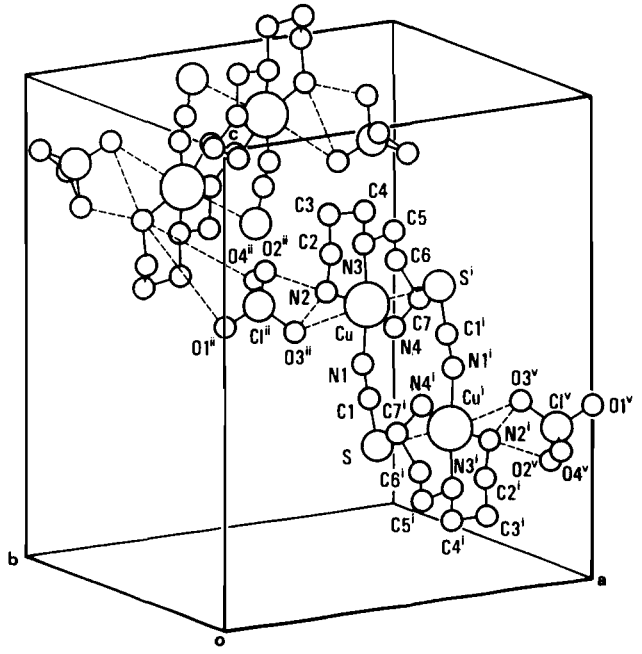

Fig. 2. The unit cell packing. Note how the ClO_4^- groups help orient symmetrically the dimeric unit through H bonds between the oxygen's electron lone pairs and the dpta's hydrogen atoms.

ligand and this is reflected also in the H bonds they form.

4.5. Crystal packing

Some details of the unit cell shown in Fig. 2 have been already discussed. It is evident from this discussion that the ClO_4^- groups pack the dimeric units by playing their dual role – semi-coordination to Cu^{II} and H bonds to the coordinated dpta ligands.

4.6. Molecular structure of $[Cu(dpta)]^{2+}$ and $[Cu(dpta)(NCS)]^+$ units calculated by molecular mechanics

We shall consider first the $N(CH_2)_3N$ fragment of the dpta ligand which is in fact part of the 1,3-propylenediamine molecule. Its conformers with metal ions have been studied in detail [25,27–29]. The three known six-membered chelate rings are the chair, boat and skew boat (Fig. 3). The relative stability order is [25,27]: chair > skew boat > boat.

We shall now build the Cu–dpta group by joining two $H_2NCH_2CH_2CH_2NH_2$ fragments and coordinating them to a common centre Cu^{II}. There are six different combinations, as found for the $[Co^{III}(dpta)_2]^{3+}$ compound [30], namely chair–chair; chair–skew boat; chair–boat; skew boat – skew boat; skew boat–boat; boat–boat.

The two rings can be combined at different angles and depending on the orientational parameters *l*-skew, *d*-skew etc. are obtained according to the signs of the CuNCC angles. Further, *mer* or *fac* isomers can be formed [25]. Fig. 4 shows these isomers as obtained by MM geometry optimization with the bond lengths Cu–N, NN and the angle NNN fixed to the respective values in Table 4.

Some MM results about the $[Cu(dpta)]^{2+}$ unit have already been reported [2]. Table 4 lists the data for the six lowest energy conformers. It is readily seen that our MM results reproduce the known conformer stability order [25], namely, chair–chair > chair–skew boat > chair–boat > skew boat–skew boat > skew boat–boat > boat–boat.

By comparing the CuNCC angles of the calculated chair–chair conformer with those of the $[Cu(dpta)]^{2+}$ unit in the dimeric compound the following points can be made.

(a) The lowest energy conformer is chair–chair (kk′ in our previous notation [2]). In general the combinations with one chair conformer are much more stable than those without such a conformer.

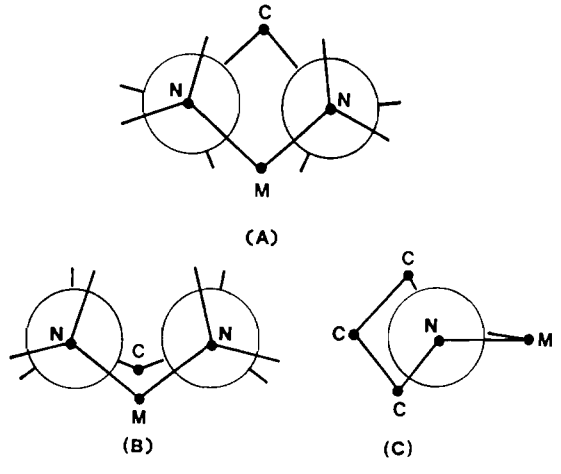

Fig. 3. The three possible conformers of a $Cu[N(CH_2)_3N]$ unit: (a) chair, (b) symmetric boat, (c) symmetric skew boat. The three conformers can be discerned by the sign of the two CuNCC dihedral angles. For (a) the angles have opposite signs, for (b) they are zero or close to zero with opposite signs, and for (c) they are of equal sign. (a) and (b) are drawn viewed down the C–N bonds, while (c) is drawn along the NN line (eclipsed Ns).

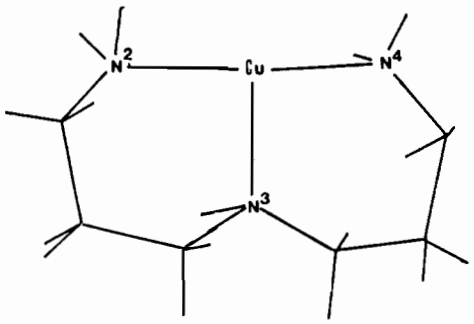

MER

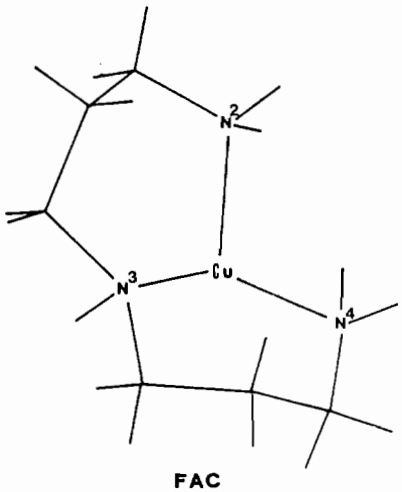

FAC

Fig. 4. The meridional (*mer*) and facial (*fac*) coordination of the dpta ligand to Cu. Note that the conformations of both rings in the *fac* isomer are skew boats while in the *mer* isomer they are both chairs.

(b) In the absence of other ligands the chair–chair dpta ligand in the stripped $[Cu(dpta)]^{2+}$ unit (No. 6) is greatly expanded – the MM calculated dihedral angles are greater than the experimental ones.

(c) The MM calculated NCuN angle (127°) of the lowest energy chair–chair conformer (No. 6) is closer to the NCuN value in the *fac* isomer (90°) than to that in the *mer* isomer (180°).

(d) Two chair–skew boat conformers (Nos. 4 and 5) come very close in energy to the chair–chair conformer (No. 6) with energy differences of 1–3 kcal mol^{-1}. The NCuN angles for these conformers are (151–165°) much closer to the *mer* isomer (180°) than to the *fac* isomer (90°).

(e) The conformer suited best to adopt *fac* coordination is skew boat–skew boat (No. 1 in Table 4). The primary amine N's lone electron pairs were found to be oriented closer the the N–Cu line in the *fac* isomer than in the *mer* isomer but the strain in the chelate rings rises steeply upon folding along the Cu–N(sec. amine) bond and conformational changes do occur during the *mer–fac* conversion.

(f) The last column in Table 4 gives the Cu^{II} HN(sec. amine) distance which is the major factor contributing heavily to the repulsion energy.

It is seen that the lowest energy chair–chair conformer has the shortest Cu···HN distance and that by folding around Cu–N(sec. amine) this distance slightly increases (HN(sec. amine)Cu angle also increases) generating a drop in repulsion energy that partially compensates for the increased repulsion energy elsewhere in the ring. This Cu···HN distance may not be of primary importance in the case of a stripped $[Cu(dpta)]^{2+}$ fragment. However, its importance most certainly rises when other ligands are also coordinated to Cu^{II}.

While (a) and (b) need no explanation, (c) certainly is intriguing. The explanation lies in the fact that both chairs have a common line CuN(sec. amine) and hence the two primary amine nitrogens avoid staying on a straight line with the Cu^{II} atom. Folding around Cu–N(sec. amine) helps reduce the strain in the upper (NCuN) part and also in the lower parts of the chairs (CCC) by making them point in different directions.

Points (d) and (e) indicate that the conformers cluster with respect to their strain energy: the chair–chair (No. 6), and two chair–skew boat (Nos. 5 and 4) form the lowest energy cluster. A chair–boat (No.3), and a third chair–skew boat (No. 2) form a higher strain energy cluster separated by about 20 kcal mol^{-1} from the first one. The boat–skew boat conformer (No. 1) forms a cluster by itself at 30 kcal mol^{-1} higher.

It may be concluded that by keeping one ring in a strictly chair conformation one may vary substantially the geometry of the other ring within the limits of a given cluster without much energy loss. This finding explains why the two dpta chelate rings could be made inequivalent in the unit cell via intermolecular contacts obviously without much loss of energy.

Table 5 lists two cases of $[Cu(dpta)]^{2+}$ with one NCS^- attached both ways. It is readily seen that:

(a) the compound with the N-coordinated NCS has a lower MM energy (about 22 kcal mol^{-1}) than the S-coordinated;

(b) the introduction of NCS^- into the Cu^{II} coordination sphere affects essentially the space taken up by dpta and also its geometry:

(i) the CuN^ACC dihedral angles are smaller by about 10° as compared with those in the $[Cu(dpta)]^{2+}$; the CuN^ICC angles remain almost unchanged (I stands for the secondary amine N);

(ii) the Cu–N(dpta) bond lengths increase upon NCS coordination in order to accommodate the incoming ligand.

While all these conclusions are easy to understand, a disturbing feature was observed: the MM calculations with $[Cu(dpta)(NCS)]^+$ showed a marked tendency of NCuN angles with neighbouring nitrogens to become higher than 90° – a value that is required for the square

Table 4
The six lowest energy conformers of the $[Cu(dpta)]^{2+}$ unit (angles in degrees, distances in Å, energies in kcal mol^{-1})

Conformer	CuNCC[a]	NCuN[b]	NN[c]	NNN[d]	MM[e]	SE[e]	TOR[f]	Cu–H[g]
1. Skew boat	42/+31	104	2.52	62	30.3	48.6	5.31	2.18
Skew boat	−74/−56		2.66					
			2.68					
2. Skew boat	68/+67	149	2.70	75	6.6	24.9	3.03	2.19
Chair	56/−60		2.73					
			3.30					
3. Boat	5/−2	177	2.54	91	3.7	22.1	6.12	2.11
Chair	−38/+30		2.48					
			3.90					
4. Chair	54/−78	165	2.69	84	3.5	3.6	4.87	2.20
Skew boat	−61/−62		2.51					
			3.48					
5. Skew boat	−19/−29	156	2.59	80	1.1	1.2	5.14	2.09
Chair	−52/+17		2.73					
			3.42					
6. Chair	59/−79	127	2.43	86	0.0	0.0	3.64	
Chair	−72/+60		2.46					
			3.33					
7. Chair	58/−59	164	3.00	85	experimental			
Chair	−47/+50		2.89					
			3.98					
8. Meridional	60/−60	180	2.82	90	hypothetical[h]			
Chair–chair	−60/+60		2.82					
			4.00					
9. Facial	60/+60	90	2.82	60	hypothetical[h]			
Skew boat	−60/−60		2.82					
Skew boat			2.82					

[a]The two rows refer to the two rings. In the first row the first number is $CuN^{A}CC$ while the second number is $CuN^{I}CC$ for the first ring. The second row gives the dihedrals for the second ring in the same sequence. N^{A} is the primary amine N, while N^{I} is the secondary amine N.

[b]The $N^{A}CuN^{A}$ angle.

[c]The first two NN distances refer to N(prim. amine)–N(sec. amine) while the third row value refers to the N(prim. amine)–N(prim. amine) distance. MM calculated Cu–N distances are systematically lower by about 0.1.

[d]The $N^{A}N^{I}N^{A}$ angle.

[e]The MM and strain energy (SE) of the lowest energy conformer are taken as reference zeroes.

[f]The torsional energy in kcal mol^{-1}.

[g]The Cu–HN(sec. amine) distance.

[h]Calculated with R(Cu–N) = 2.00 Å.

planar arrangement. Thus a trend from planar towards a pseudotetrahedral CuN_4 unit was detected. This is easily explained by invoking the absence of electronic factors in the MM calculations; exactly such factors are essential for Cu^{II} to make it adopt a square planar arrangement of its ligands [31]. For this reason the values listed in Table 5 should be viewed with caution.

Other arguments apply to the dimeric $[Cu(dpta)(NCS)]_2^{2+}$ unit: MM calculations gave two separate $[Cu(dpta)(NCS)]^{+}$ units which were reluctant to make the contacts required to form a dimer: the Cu–S contact of two neighbouring units stayed very long (>5 Å). This is also an indirect proof that the factors shaping the symmetric dimer are the intermolecular contacts (see also Section 4.8).

4.7. MNDO calculations of the free DPTA ligand

To glimpse at the changes of the dpta ligand that had occurred upon coordination we have initiated a full MNDO geometry optimization taking as input the structure of the coordinated ligand from Table 3 and letting it distort freely. This is the reverse of what happens upon coordination. The calculations gave $\Delta H_f = +30$ kcal mol^{-1} for the coordinated ligand prior to optimization and -10.39 kcal mol^{-1} after geometry optimization with dpta keeping its chair–chair conformation but changing some bonds and mainly opening some angles (vide infra). Hence about 40 kcal mol^{-1} are lost in conformational energy upon coordination.

Table 5
The geometries of the $[Cu(dpta)NCS]^+$ and $[Cu(dpta)SCN]^+$ units obtained by molecular mechanics

Unit	CuNCC (°)	CuNCS[a] (°)	NN (Å)	MM[b] (kcal mol^{-1})
$[Cu(dpta)NCS]^+$	60/−66	159 N	3.02	0.0
chair–chair	−47/+50		2.86	
			3.80	
$[Cu(dpta)SCN]^+$	19/−29	117 S	2.46	22.3
chair–chair	−38/+43		2.83	
			3.76	
Experimental	58/−59	167 N	3.00	
chair–chair	−47/+50	95 S	2.89	
			3.98	

[a]The angles CuNC (N) or CuSC (S), respectively.
[b]The MM energy of the N-coordinated unit is taken as reference zero.

The major displacements during the optimization process were read out from the internal coordinate derivative values. They occur with the N(sec. amine) atom and the C atoms attached to it. Valence angles opened (2–20°) to let the strain energy decrease; bond lengths increased (by 0.01–0.02 Å) and dihedral angles expanded (3–15°) and these changes took second place with equal energy-lowering contributions. Although the greatest changes occurred with the dihedral angles, their contribution to lowering the energy of the uncoordinated ligand was equal to that of the bond length variations.

The charges on the N atoms of the geometry-optimized dpta ligand were q(N(prim. amine)) = −0.27 and q(N(sec. amine)) = −0.33. This is a clear indication that were it not for the big strain involved in positioning the secondary amine N close to Cu, its bond to Cu^{II} would have been stronger than that of the primary amine's nitrogens.

4.8. Electronic structure of $[Cu(dpta)(NCS)]_2^{2+}$

4.8.1. The thiocyanate ligand

Ab initio calculations of the free NCS^- ligand with full geometry optimization gave the bond lengths NC = 1.162 Å, CS = 1.703 Å and the bond angle NCS = 180°. The charge distribution is $N^{-0.392}C^{-0.040}S^{-0.568}$, showing a high degree of electron delocalization. Judging from its charge the S atom is a slightly better donor than the N atom in the free ligand.

Using the structural parameters of the coordinated NCS^- ligand (Table 3) in the calculation (NC = 1.15 Å, CS = 1.78 Å, angle NCS = 180°) the following charge distribution was found: $N^{-0.388}C^{-0.033}S^{-0.578}$.

This structure is only richer in energy by 0.0034 eV than the optimized one. Assuming no Cu–NCS electron delocalization (pure electrostatic Cu–N bond) N-coordination reduces the charge on N and slightly increases the negative charge on S. The coordinated NCS ligand has a slightly shorter CN and a longer CS bond length than the uncoordinated implying that the resonance structure $^-N{=}C{=}S$, which predominates in the free ligand, approaches the $N{\equiv}C{-}S^-$ structure upon coordination. Both facts suggest that S becomes a slightly better donor after NCS^- is N-coordinated. Since the Cu^{II} polarization effect on NCS^- is not accounted for, this conclusion is uncertain.

4.8.2. The $[CuNCS]^+$ and $[Cu(dpta)(NCS)]^+$ units

The electronic structures of the $[CuNCS]^+$ (linear) and $[CuSCN]^+$ (bent CuSC = 90°) units were calculated with the structure parameters taken from Table 3. The charge distributions were $Cu^{1.030}N^{-0.353}C^{0.249}S^{0.075}$ and $Cu^{0.840}S^{0.198}C^{0.032}N^{-0.070}$. It is seen that the Cu–N bond is highly ionic. The Cu–S bond is more covalent than the Cu–N bond and less electron density is displaced from the ligand to the central atom in the N-coordinated than in the S-coordinated unit. The CuSCN unit because of the remaining negative charge on N may further coordinate to another Cu^{II}.

Finally, the ab initio calculations on the dimeric $[CuNCSCu]^{3+}$ and $[CuNCS]_2^{2+}$ units gave the following results

$$Cu^{1.448}N^{-0.292}C^{0.278}S^{0.346}Cu^{1.220}$$

and

$$\begin{array}{ccc} Cu^{0.898}N^{-0.300}C^{0.229}S^{0.173} & & \\ | & & | \\ S^{0.173}C^{0.229}N^{-0.300}Cu^{0.898} & & \end{array}$$

It is readily seen that the electron shift in the dinuclear unit from NCS^- to Cu^{II} is substantial but much less than for the mononuclear CuNCS unit. The two centres somehow reduce the atomic charges – the S-coordinated Cu atom reduces its charge more than the N-coordinated Cu atom. In the dimeric unit the N atom remains negative which suggests a strong electrostatic bond between N-coordinated NCS^- and the Cu atom.

When the dpta ligand is added to $[CuNCS]^+$ the resulting charge distribution in $[Cu(dpta)(NCS)]^+$ is

$$\begin{array}{ccccc} & & -0.21\mathrm{N} & & \\ & & / \ | & & \\ -0.23\mathrm{N} & - & \mathrm{Cu} & -0.20\mathrm{N}-0.72\mathrm{C}^{0.14}\mathrm{S}^{0.08} & \\ & & \backslash \ | & & \\ & & -0.21\mathrm{N} & & \end{array}$$

Hence, although similar in length the four CuN bonds are not equivalent in nature: the Cu–NCS bond is much more ionic than the Cu–N(dpta) bonds. Similar results were obtained by MNDO calculations for the free ligand – the secondary amine nitrogen is more negative than the primary amine nitrogens.

4.9. The vibrational spectrum of dpta and $[Cu(dpta)(NCS)]^+$ calculated by NCA and MOPAC

Having thus far rationalized the geometric parameters of the studied compound, it may be of interest to find manifestations of these parameters in the easily accessible vibrational spectra; spectra–structure correlations may be in general used as diagnostic tools.

The structural parameters for the dpta ligand were taken from Table 3 and consequently they refer to a coordinated ligand. The IR spectra of dpta have been taken from the Aldrich Library of FT-IR spectra [32]. The values below 400 cm^{-1} have been adopted from another work on primary and secondary amines [33]. The initial force constants were those reported for Cu–dien molecules [34].

Since the ligand geometry is that of a coordinated one and the vibrational spectrum is of a free ligand, the NCA gave rough estimates for the force constants. These constants were used as input in the NCA interpretation of the compound's vibrational spectrum.

The vibrational spectra of the free dpta ligand were treated in another way. The linear dpta geometric structure was obtained by MM optimization. This structure was input for MNDO geometry optimization and subsequently to calculate the linear dpta's vibrational spectrum with the MOPAC package.

The vibrational spectrum of a coordinated dpta ligand was calculated after: (a) MM geometry optimization of the $[Cu(dpta)]^+$ unit, (b) replacing the Cu^{II} ion with a dummy atom, (c) geometry optimization by MNDO. The chair–chair conformation and the *mer* isomer parameters were preserved in this procedure.

Both sets of calculated vibrational spectra gave lengthy tabular data, see Section 6. Some relevant parts of the spectra will be discussed here.

(a) There are a number of bands in the linear form's spectrum (773, 818, 1203, 1219, 1246, 1331, 1345 cm^{-1}) which are lacking in the *mer* isomer's spectrum. The 773, 1203, 1246 cm^{-1} bands from the above list are almost pure CC bending or stretching modes.

(b) Similarly there are a number of bands in the *mer* isomer's spectrum (402, 856, 891, 994, 1030, 1280 cm^{-1}) that are lacking in the linear form's spectrum. The 891 cm^{-1} band does not involve N atom displacements. However, in the compound's spectrum it gets some mixture of ν(CN).

(c) The experimental dpta spectrum displays bands of both (linear and *mer*) forms; however, in the *mer* form's spectrum the 1280 and 402 cm^{-1} bands are lacking and in the linear form's spectrum the bands 1203, 1219, 1246, 1331 and 1345 cm^{-1} are lacking.

The structural parameters of the dimeric compound were taken from the present X-ray diffraction study. Two ClO_4^- groups were also included in the treatment although they are semi-coordinated (vide supra).

The first step involved a separate NCA for the ClO_4^- and NCS^- groups with geometric parameters taken from Table 3. The second step was to treat the $[Cu(dpta)]^{2+}$ fragment with the initial force field, taken from NCA of the free ligand. All force constants were allowed to vary in the optimization procedure and in some cases several different assignments were tested. This fragmentation procedure was necessary in view of the large number of atoms in the dimeric compound.

Finally the entire $[Cu(dpta)(NCS)(ClO_4)]_2$ complex was treated.

The extracted force constants are listed in Table 6. It is readily seen that F(CNC) and F_t(CCCN) increase but F(NH), F(NC), F(HNH) and F(NCC) decrease upon coordination. It may be thus concluded that the distortion occurring with the ligand upon coordination is taken up mainly by the secondary amine bonds and angles.

Despite the low symmetry, the dpta's vibrational modes were not mixed with those of the ClO_4^- and NCS^- groups; the dpta frequencies proved easy to sort out from those of NCS^- and ClO_4^-. There are small differences as compared with the free dpta's spectrum exactly where expected for the groups which take part in coordination: $\nu(NH_2)$ and ν(NH) are 3360 and 3280 cm^{-1} in the free ligand and 3320 and 3266 cm^{-1} in the coordinated ligand, respectively. Some of the dpta's skeletal modes were also affected when dpta is attached at three points to Cu^{II}: $\delta_{scissor}$(HNH) (1600 cm^{-1} in the ligand) and $\delta_{wagging}$ (1126 cm^{-1}) were both shifted by 20 cm^{-1} upon coordination.

By comparing the experimental spectrum of the dimeric compound with the calculated linear and *mer* dpta forms' spectra it is seen that the 855, 890 and 980 cm^{-1} bands indicate the presence of the *mer* coordinated in the studied compound. Hence these bands may serve as a diagnostic tool to prove the dpta's *mer* coordination mode.

The ClO_4^- vibrational bands showed splittings and IR/R behaviour that are typical for C_{3v} symmetry [21]. The ν_3 mode splits into three components (1145, 1105, 1082 cm^{-1}), ν_2 splits into two components (635 and 620 cm^{-1}), ν_4 (IR 510 cm^{-1}, R 512 cm^{-1}) remains unsplit and finally ν_1 (predicted at 836 cm^{-1}) is lacking.

The NCS^- ligand gives typically very strong and characteristic absorption bands over narrow ranges of frequencies [36]. The strong IR doublet 2110 and 2065 cm^{-1} was ν_{asym}(NCS). This relative strong splitting (45 cm^{-1}) is in agreement with the bridging role of this ligand. ν_{sym}(NCS) was observed at 810 cm^{-1} and δ(NCS) at 670 cm^{-1}.

The Cu–N stretching modes were widely distributed due to the low symmetry. The IR bands at 300, 340, 355 and 410 cm^{-1} were found to have high contribution from ν(CuN). The 144, 181 and 216 cm^{-1} bands contain

Table 6
Force constants for free dpta and the complex extracted by normal coordinate analysis and used in MM calculations

Definition	Free dpta	Complex	MMX[a]	Definition	Complex	MMX[b]
F(CH)	4.528	4.579	4.60	F(CuN)(NH)	1.174	0.89
F(NH)	6.048	5.997	6.10	F(CuN)(NH)	1.111	0.89
F(CN)(NH_2)	5.056	5.336	5.10	F(CuN)(NCS)	2.288	2.00
F(CN)(NH)	3.927	3.632	3.89	F(CuS)	0.829	0.50
F(CC)	3.526	3.428	4.40	F(CuO)	0.257	0.89
F(HNH)(NH_2)	0.631	0.608	0.50	F[(H_2)NCuN(NCS)]	0.625	
F(CNC)	0.834	1.090	0.63	F(CuOCl)	0.011	
F(NCC)	0.380	0.291	0.57	F[CuNC(S)]	0.439	
F(CCC)	0.183	0.193	0.45	F[CuN(H_2)C(NH_2)]	0.439	
F(HNH)(NH)	0.534	0.535	0.50	F(CuNC)(NH)	0.439	
F(CCH)(CCH_2C)	0.575	0.584	0.36	F(CuSC)	0.572	
F(CCH)(C-CH_2-N)	0.612	0.618	0.61	F(OCuN)(NH_2)	0.248	
F(HNC)(NH)	0.368	0.374	0.28	F(OCuN)(CS)	0.248	
F(HNC)(NH_2)	0.175	0.176	0.18	F(OCuN)(NH)	0.248	
F(NCH)(NH_2)	0.641	0.623	0.50	F(SCuN)(NH_2)	0.213	
F(NCH)(NH)	0.636	0.694	0.65	F(SCuN)(NH)	0.213	
F(CC-t)(CCCN)	0.137	0.155		F(SCuN)(CS)	0.213	
F(CC-t)(NCCC)	0.510	0.638		F(NCuOCl-t)	0.173	
F(CN-t)(CCNC)	0.138	0.148		F(OClOCu-t)	0.173	
F(CN-t)(HNCC)	0.099	0.099		F(CSCuN-t)	0.173	
F(CN/CN)(NH)	−0.024	−0.022		F(ClO)	6.553	
F(CCH/CCH)	−0.066	−0.065		F(OClO)	1.720	
F(CN/CN)(NH_2)	0.460	0.261		F(N=C)	15.539	
F(NH/NH)(NH_2)	−0.096	0.037		F(C=S)	4.054	
F(CN/NCH)(NH_2)	−0.151	−0.090		F(N=C=S)	2.556	
F(CC/CCH)	−0.097	−0.148				

Stretching force constant in mdyn $Å^{-1}$; bending force constants in mdyn rad^{-1}.
[a]From the MMX param. out file.
[b]From ref. [21]; the values differ from those of Ref. [35].

considerable contribution from δ(NCuN). The 258 cm^{-1} band is δ(NCS).

5. Conclusions

The structure of the dimeric compound [Cu(dpta)(NCS)(ClO_4)]$_2$ is quite similar to the one with dien as ligand [6]. Both structures are dimeric and they differ from the corresponding nitrate compounds, which are monomeric. The formation of the dimeric unit is mainly due to crystal packing requirements which are governed by the peculiar role of the ClO_4^- ions. These ions form both intermolecular contacts with Cu^{II} (semi-coordination) and H bonds to dpta's hydrogens. In the nitrate compounds one NO_3^- ion is remote (Cu–O contact >5 Å) and it cannot participate in H bonds.

The conformational analysis of uncoordinated and coordinated dpta shows that although the chair–chair conformation of coordinated dpta is the most stable one, there are also other dpta conformers that are close in energy. The dpta distortions to make its two chairs inequivalent are essential in accommodating the ClO_4^- ion in the unit cell and they can occur with practically very little rise of strain energy.

6. Supplementary material

Two tables with the experimental and calculated vibrational frequencies of the free dpta ligand and of the studied compound (4 pages) are available upon request. Tables of anisotropic displacement parameters, all hydrogen atoms parameters, intra- and intermolecular atomic distances, valence angles and torsion angles (5 pages) are also available from the authors.

Acknowledgements

Partial financial support through Grant No. 136 of the Bulgarian National Science Fund is acknowledged. One of us (G.S.N.) is grateful to the EEC's Science Directorate for a fellowship which made possible his stay in Thessaloniki to complete this work.

References

[1] (a) K.D. Karlin and J. Zubieta (eds.), *Copper Coordination Chemistry: Biochemical & Inorganic Perspectives*, Adenine, New York, 1983; (b) H. Sigel (ed.), *Metal Ions in Biological Systems*, Vol. 13, *Copper Proteins*, Marcel Dekker, New York, 1981.

[2] G. Gliemann, U. Klement, C. Stuckl, C. Bolos, G. Manoussakis and G. St. Nikolov, *Inorg. Chim. Acta, 195* (1992) 227.
[3] M. Cannas, G. Carta and M. Marangiu, *Gazz. Chim. Ital., 104* (1974) 581.
[4] M. Cannas, G. Carta and M. Marangiu, *J. Chem. Soc., Dalton Trans.,* (1976) 550.
[5] A. Cristini and G. Ponticelli, *J. Inorg. Nucl. Chem., 35* (1973) 2691.
[6] M. Cannas, G. Carta and G. Marongiu, *J. Chem. Soc., Dalton Trans.,* (1974) 556.
[7] M. Cannas, G. Carta and G. Marongiu, *J. Chem. Soc.,* (1974) 553.
[8] M. Cannas, G. Carta and G. Marongiu, *J. Chem. Soc., Dalton Trans.,* (1973) 251.
[9] F.S. Stephens, *J. Chem. Soc. A,* (1969) 883.
[10] R. Allmann, M. Krestl, C. Bolos, G. Manoussakis and G.St. Nikolov, *Inorg. Chim. Acta, 175* (1990) 255.
[11] R. Barbucci, P. Paoletti and G. Ponticelli, *J. Chem. Soc. A,* (1971) 1638.
[12] S.R. Hall and J.M. Stewart, *XTAL System of Crystallographic Programs,* Version 3.0, Crystallography Centre, University of Western Australia and Chemistry Department, University of Maryland, USA, 1990.
[13] D.T. Cromer and J.B. Mann, *Acta Crystallogr., Sect. A, 24* (1968) 321.
[14] *International Tables for X-ray Crystallography,* Vol. IV, Kynoch, Birmingham, UK, 1974.
[15] H.D. Megaw, *Crystal Structures: A Working Approach,* Saunders, Philadelphia, PA, 1973, p. 502.
[16] R. Koch and B. Wiedel, *MOPAC 6.0 for the IBM-PC QCMP113,* Bloomington, IN, USA.
[17] M. Dupuis, D. Spangler and J.J. Wendoloski, *GAMESS,* Program QG01, National Resource for Computations in Chemistry, Software Catalog, University of California, Berkeley, CA; M.W. Schmidt, K.K. Baldridge, J.A. Boatz, J.H. Jensen, S. Koseki, M.S. Gordon, K.A. Nguen, T.L. Windus and S.T. Elbert, *QCPE Bull., 10* (1990) 52–54.
[18] N.L. Allinger, *MM2 J. Am. Chem. Soc., 49* (1977) 8127; *QCPE* No. 395, Bloomington, IN, USA; J.J. Gajewski and K.E. Gilbert, *MMX,* Indiana University, USA.
[19] (a) R.D. Hancock, *Prog. Inorg. Chem., 37* (1989) 187; (b) P. Comba, *Coord. Chem. Rev., 123* (1993) 1, and refs. therein.
[20] G.R. Brubaker and D.W. Johnson, *Coord. Chem. Rev., 53* (1984) 1.
[21] G. Bauer and H. Mikosch, *Program for Normal Coordinate Analysis,* Technical University, Vienna, 1989.
[22] D.S. Brown, J.D. Lee, B.G.A. Melson, B.J. Hathaway, I.M. Procter and A.A.G. Tomlinson, *J. Chem. Soc., Chem. Commun.,* (1967) 369.
[23] B.J. Hathaway and A.E. Underhill, *J. Chem. Soc.,* (1961) 3091.
[24] T.R. Felthouse and D.N. Hendrickson, *Inorg. Chem., 17* (1978) 444.
[25] C.J. Hawkins, *Absolute Configuration of Metal Complexes,* Wiley-Interscience, New York, 1971.
[26] A.F. Wells, *Structural Inorganic Chemistry,* Clarendon, Oxford, 1984, p. 405.
[27] F.A. Jurnak and K.N. Raymond, *Inorg. Chem., 11* (1972) 3149.
[28] S.R. Niketic, K. Rasmussen, F. Woldbye and S. Lifson, *Acta Chem. Scand., Ser. A, 30* (1976) 485.
[29] J.R. Gollogly and C.J. Hawkins, *Inorg. Chem., 11* (1972) 156.
[30] T.W. Hambley, G.H. Searle and M.R. Snow, *Aust. J. Chem., 35* (1982) 1285.
[31] I.B. Bersuker, *The Jahn Teller Effect and Vibronic Interactions in Modern Chemistry,* Plenum, New York, 1984.
[32] *The Aldrich Library of FT-IR spectra,* Vol. 1, London, 1st edn., 1970, p. 310(B).
[33] J.E. Stewart, *J. Chem. Phys.,* (1950) 1269.
[34] N.S. Trendafilova, G.St. Nikolov, G. Bauer and R. Kellner, *Inorg. Chim. Acta, 210* (1993) 77.
[35] P.V. Bernhardt and P. Comba, *Inorg. Chem., 31* (1992) 2638.
[36] B.J.H. Clark and C.S. Williams, *Spectrochim. Acta, 22* (1966) 108.